International Journal of Advanced Trends in Engineering and Technology (IJATET)
International Peer Reviewed - Refereed Research Journal, Website: www.dvpublication.com
Impact Factor: 5.965, ISSN (Online): 2456 - 4664, Volume 10, Issue 1, January - June, 2025

COMPUTING AND PREDICTING THE VEGETATION COVER USING NDVI UNDER THE CONDITIONS OF CLIMATE CHANGES, FOR THE PERIOD 2000 - 2024: A CASE STUDY, KARBALA CITY, IRAQ

Rusul A Al-Ameri*, Noor Sabah & Ghufran Ahmed Jawad Al-Baaj*****
* Najaf Technical Institute, Al-Furat Al-Awsat Technical University, Najaf, Iraq
** Ministry of Education, Iraq
*** Department of Aviation Techniques, Najaf Technical Institute, Al-Furat Al-Awsat Technical University, Najaf, Iraq

Cite This Article: Rusul A Al-Ameri, Noor Sabah & Ghufran Ahmed Jawad Al-Baaj, "Computing and Predicting the Vegetation Cover Using NDVI Under the Conditions of Climate Changes, for the Period 2000 - 2024: A Case Study, Karbala City, Iraq", International Journal of Advanced Trends in Engineering and Technology, Volume 10, Issue 1, January - June, Page Number 5-12, 2025.

Abstract:

Vegetation cover plays a vital role in aiding to get rid of the atmospheric dust and harmful suspensions, so it can be considered as one of the most important factors affecting the ecosystem. Also, it reduces the differences in temperatures between days and nights, making the temperature more appropriate for living. Cycles of minerals, organic elements, water (including rain), and moisture are all affected by the vegetation cover. For this work, the Normalized Difference Vegetation Index (NDVI) is computed relying on images from the website of the United States Geological Survey (USGS) for Landsat7 ETM+ (Enhanced Thematic Mapper Plus) and Landsat 8OLI (Operational Land Imager) satellites. The data of February months for the years 2000, 2014, and 2024 are chosen to calculate the green areas for the holy Karbala city utilizing the Geographic Information System software (GIS 10.3). Weather data from Nasa power data are used as well for the period (1995- 2024). Results from satellite images show that the vegetation cover has been increased by 245% from 2000 to 2014, and for the same period, the average percentage of precipitation amount is estimated to increase by 153%. The rainfalls were more concentrated on the eastern, northeastern, and southeastern sides of the city.

Likewise, the period extending from the year 2015 to 2024 has witnessed a very large increase in vegetation areas by (37,750 %) in the western and eastern parts of the city because of 274% increase in the precipitation, and the projects that are adopted to convert desert areas into green agricultural areas by Holy Abbasid Shrine. For the future, the HadGEM2-rcp26 climate model was used, and the areas of vegetation cover were calculated for the periods (2024-2050, 2050-2070, and 2070-2080) in general, the area of vegetation to enhanced mean annual precipitation and decreased annual temperature for the period 2050-2080. Linear regression in was used to forecast vegetation cover. Data were analyzed through scatter plots and a fitted linear trend line, resulting in a predictive equation. The findings reveal a significant correlation, demonstrating the effectiveness of linear regression as a tool for forecasting vegetation cover based on rainfall.

Key Words: Climate Change, ETM+, Forecasting, Karbala City, Landsat Image, NDVI, Vegetation Cover

Highlights:

- NDVI Calculation: The Normalized Difference Vegetation Index (NDVI) was calculated using Landsat 7ETM+ and Landsat 8OLI satellite images for Karbala from 2000 to 2024, using Geographic Information System (GIS) software.
- Future Projections Using the HadGEM2-rcp26 Model: A climate model was used to forecast increases or decreases in precipitation and temperatures and their impact on vegetation cover for the periods 2024-2050, 2050-2070, and 2070-2080.
- Statistical analysis, particularly linear regression, was used to clarify the relationship between vegetation cover and rainfall rates, contributing to a deeper understanding of climate impacts and planning sustainable agricultural initiatives in the future.

1. Introduction:

The need for spatially detailed forecasts of potential vegetation under rising atmospheric CO_2 has emerged in response to the growing scientific and public concern about global environmental change and its effects on terrestrial ecosystems. [1]. It is anticipated that maps derived from these projections will show the probable effects of global warming on animals, natural vegetation, and forestry and agriculture [2].

As known, the amount of plant cover is essential to the terrestrial ecosystem's health, so it can be considered the most important index as a hub connecting changes in the climate, atmosphere, water, and soil. However, human activities may positively or negatively affect vegetation cover. Expansion of cities at the expense of green lands, deforestation, and desertification fall under harmful human activities. In contrast, positive human activities, such as planting arid zones and increasing green lands inside and around cities, are related to the stability of the local and global ecosystem. The trend in both harmful and useful changes is a main indicator for judging the situation of the ecosystem.

To monitor these alterations in vegetation cover, it is necessary to record changes at regular intervals to provide valuable information about vegetation area sizes. Satellite-based remote sensing is employed as an affordable way to provide the necessary data for vast geographical areas [3]. It remains a dilemma in watershed management to efficiently quantify vegetation cover changes over long terms. This data can offer complete information to comprehend land-atmosphere interactions and their consequences on global ecosystems. Also, natural effects, such as plant transpiration, surface albe do, emissivity, and roughness, influence vegetation cover and, consequently, surface water and energy budgets [4]. Several regions globally are dry or semi-arid, including the Middle East, the one that is more susceptible to the consequences of climate change, visible in many countries (e.g., Saudi Arabia, Sudan, Qatar, Syria, Iran, Kuwait, Turkey, and Iraq) [5]. These changes are linked to drought, inland floods, heat stress, large rainstorms, restricted water supplies, agriculture, and food security [6].

The Normalized Difference Vegetation Index (NDVI) is probably the most widely used remotely sensing spectral indicator to tracking Earth's land surface [7]. Climate change phenomena such as temperature, precipitation, and radiation contribute to changes in vegetation cover sizes [8]. Elevated atmospheric CO2 concentrations and shifting nitrogen deposition rates also have the same influence [9]. Authors observed that vegetation dynamics have grown according to variations in vegetation lands monitored through earth-observing satellite data [10]. By the end of the twenty-first century and beyond, cumulative CO2 emissions will determine the mean surface warming based on the Fifth-Assessment - Report (AR5) by the Intergovernmental Panel on Climate Change (IPCC) [11]. To characterize greenhouse-gas (GHG) emission, four representative concentration pathways (RCPs) are established, with these models used to evaluate the expenses associated with cutting emissions along specific concentration pathways. The RCP2.6 scenario aims to maintain global warming above the pre-industrial temperature by less than 2°C as a stringent mitigation scenario, while RCP4.5 and RCP6.0 are considered intermediate, and RCP8.5 represents extremely high GHG emissions. Projected increases in the global mean surface temperature range from 0.3°C to 4.8°C within the twenty-first century, depending on the evaluated emission scenarios [12].

According to the related works above, Iraq has no comprehensive studies in the literature covering its entire area to show either growth or reduction in vegetation cover. Karbala City will be the focus of this research. Therefore, in this paper, Landsat8OLI and Landsat7ETM+satellite images will be used to compute the Normalized Difference Vegetation Index (NDVI) for 2000, 2014, and 2024, using Geographic Information Systems software (GIS 10.3) with weather data (precipitation and temperatures) from NASA Power Data for the period (1995-February 2024), which is effective in creating weather data sets in the absence or inaccessibility of ground weather station data [13].

Additionally, the HadGEM2-rcp26 model was used to forecast weather data involving minimum and maximum temperatures and precipitation for the future period (2024-2080) for Karbala Governorate. Forecasted data used correlation and trend analyses to assess how vegetation is affected by climate change.

2. Study Area:

Karbala is an Iraqi city, located in the Middle Euphrates region. Its population reached about 1,350,577 according to 2020 estimates, making it the seventh most populous city in Iraq. The capital of the Karbala Governorate is the city of Karbala in central Iraq. It is situated between latitudes 32° 37′ 0″ N and longitudes 44° 2′ 0″ E, approximately 110 kilometers southwest of Baghdad [14], whereas the total area is roughly 40,669 ha [15]. Its population reached about 1,350,577 according to 2020 estimates, making it the seventh most populous city in Iraq. The city is 30 meters above sea level, located at a longitude of 44° 40' and a latitude of 33° 31' [16]. Administratively, Karbala Governorate includes three districts (Karbala, Ain Altamur, Al-Hindiya) [17]. Karbala is bordered by Baghdad from the north, by Najaf from the south, by Hilla from the southeast, and by Anbar to the north and to the west, as shown in figure 1 [18].

Figure 1: Location of Karbala Governorate in Iraq [22].

3. Material and Method:

Two different kinds of data were gathered for this work: climate data (precipitation and temperatures) from the site of NASA Power Data [19] for period started from 1995 to February of 2024. The second type of data is remote sensing data, which includes satellite images (Landsat 8OLI and Landsat 7ETM+), taken from the website of the United States Geological Survey (USGS) [20] for the years 2000, 2014, and 2024. As for future data, it was downloaded from the Inter-Sectoral Impact Model Inter comparison Project (ISIMIP) RCP2.6 scenario for the period 2024-2080.

Figure 2 shows the annual average precipitation for the period 1995-2023, and figure 3 illustrates the annual maximum and minimum temperatures for the period 1995-2023.

International Journal of Advanced Trends in Engineering and Technology (IJATET)
International Peer Reviewed - Refereed Research Journal, Website: www.dvpublication.com
Impact Factor: 5.965, ISSN (Online): 2456 - 4664, Volume 10, Issue 1, January - June, 2025

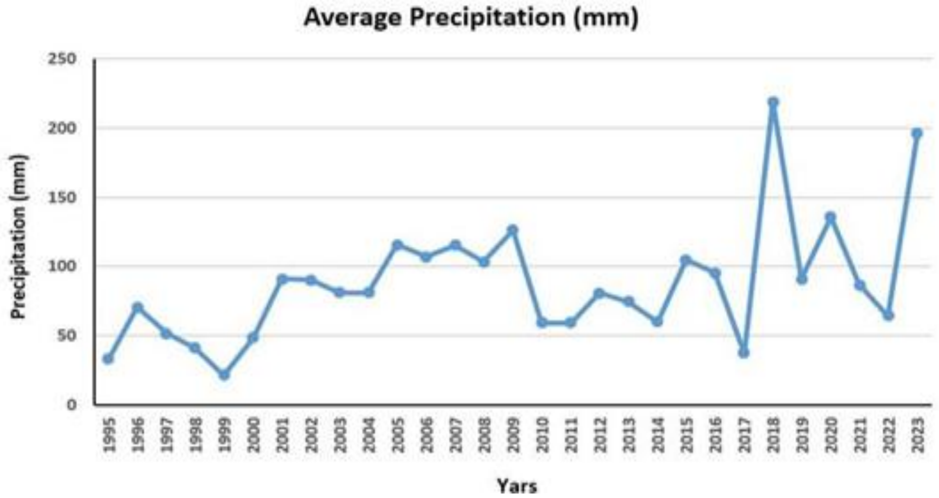

Figure 2: Annual average precipitation for the period (1995-2023)

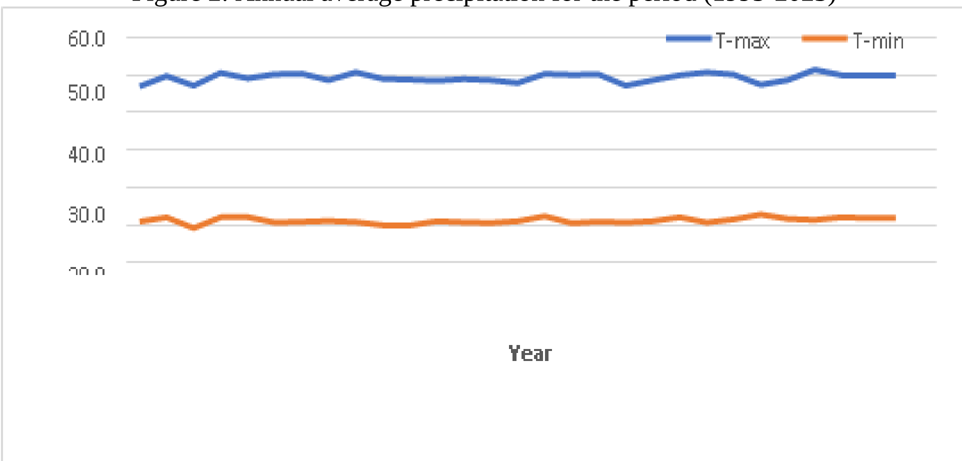

Figure 3: Annual average maximum and minimum temperature for the period (1995-2023)

Method of forecasting vegetation consist of many steps:

- Data Preparation: In this study, historical data for rainfall and vegetation cover was collected. The dataset consists of two primary columns: "Rainfall" (measured in millimeters) and "Vegetation Cover" (expressed as a percentage). This data was organized in an Excel spreadsheet, where each row corresponds to a specific time period.
- Scatter Plot Creation visually assess the relationship between rainfall and vegetation cover, a scatter plot was generated: The data was selected, and the "Insert" tab in Excel was utilized to create a scatter plot. An illustration of the relationship between the two variables is shown by this plot, allowing for an initial evaluation of the relationship.
- Trend line Addition: To quantify the relationship, a linear trend line was applied:
- By right-clicking on any data point within the scatter plot and selecting "Add Trend line," the linear regression model was fitted to the data. In the trend line options, the "Linear" model was chosen. Additionally, The "Display R-squared value on chart" and "Display Equation on chart" options were activated. Usually, the resultant equation looks like this:

$$Y = mx + by = mx + by = mx + b \quad (1)$$

- Where y represents vegetation cover, xxx is rainfall, mmm is the slope of the line, And the y-intercept is bbb. The percentage of variance in plant cover that can be attributed to rainfall is shown by the R-squared value.

3.1 Normalize Difference Vegetation Index:

Vegetation indices are employed in many remote sensing studies to investigate vegetation, the normalized difference vegetation index (NDVI) is among the most often used vegetation indexes, and during the past 20 years, it has been amply shown to be useful for satellite evaluation and monitoring of the world's plant cover [21]). NDVI is described as:

$$NDVI = NIR - Red \,/\, NIR + Red \quad (2)$$

Where NIR and Red are measures of reflectance (or spectral radiance) taken using sensors in the NIR and red (visible) bands, respectively [22]. Table (1) shown the NDVI values for various characteristics [23].

Table 1: NDVI values for various characteristics

Features	NDVI Values
Water (Deep and Shallow)	-0.41379 to -0.10401
Built Ups / River Sand	-0.10401 to 0.055727
Fallow/ Wasteland	0.055727 to 0.20579
Crop, Grass	0.20579 to 0.37035
Agro Forestry	0.37036 to 0.51073
Forest	0.51074 to 0.82051

For Landsat7 data, NDVI=(Band4-Band3)/(Band4+Band3). (2)

For Landsat8 data, NDVI=(Band5-Band4)/(Band5+Band4) [24] (3)

4. Results and Discussion:

4.1 NDVI and Effect of Climate Condition on Vegetation Cover:

4.1.1 For the Period (1995-2000):

During the period from 1995 to 2000, the value of annual rainfall ranged from 70.7 mm to 21 mm, while the results of the NDVI were given through Landsat 7ETM+ satellite images, as shown in the Table below. The area and percentage of plant cover as well as other parameters for the year 2000 are displayed in table (2):

Table 2: The area and percentage of vegetation cover and other features

Features	Area (km²)	% Percentage
Water	22.00515	13.3444
Wasteland / Fallow	140.05326	84.9312
Grass / Crop	2.84103	1.72286
Forest	0.00267	0.001619

From the table above it shows that the percentage of vegetation cover represents 1.724 % of the governorate's area, which represents a very small area, while the Fallow / wasteland occupied the largest percentage of the governorate's area, at 84.9 %, with an area of 140 km², followed by the water area, which constituted a percentage of 13.3. Figure (3) shows the spatial distribution of vegetation cover and other features. Whereas the vegetation cover is distributed in the northeastern side of the governorate, and this part is where the rainfall amounts were concentrated, as in Figure (3b) which shows the distribution of rain over the governorate, while the average maximum temperatures ranged between (47.02 to 50.38) C°, and the minimum temperatures ranged from (15.7 to 17.2) C°, distributed over the governorate, as in Figure (4c, d), which shows the distribution of max. and min. temperatures in the governorate, with the eastern, northeastern, and southeastern parts being the hottest compared to the rest of the parts.

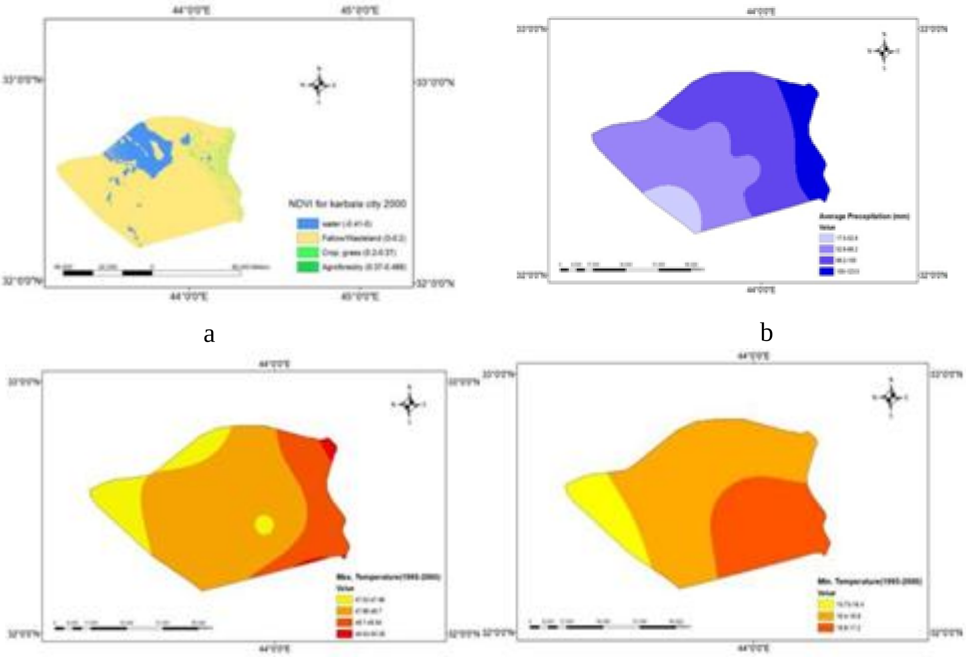

a b

c d

Figure 4 (a, b, c, and d) the distribution of vegetation cover, precipitation, and maximum and minimum temperatures for Karbala Governorate

4.1.2 For the Period (2001-2014):

In the period from 2001 to 2014, the results of the NDVI for year 2014 from Land sat 8 OLI satellite images showed that the areas of vegetation cover increased at a rate of 245 % over the previous period, Table (3) displays the area, percentage, and other characteristics of vegetation cover for the years 2001-2014:

Table 3: The area covered by vegetation, its proportion, and other characteristics during the years 2001-2014

Features	Area (km²)	% Percentage
Water	7.51896	4.563051
Waste land / Fallow	151.32609	91.835658
Grass / Crop	5.92083	3.59319
Forest	0.01335	0.008102

From the table above, it is clear that the vegetation cover has increased in area, covering approximately 3.6 % of the governorate's area compared to what it was in the year 2000. It is worth noting that the average amounts of precipitation ranged between (25.61-198.6) mm, that is, the increase in the average annual precipitation amounts is approximately 153% compared to the previous period and the largest amounts were concentrated in the eastern, northeastern, and southeastern parts of the governorate. Which contained the largest percentage of vegetation cover, while the maximum and minimum temperatures ranged between (47.28-50.62) and (10.04-11.25) C° respectively, that is, the increase in maximum temperatures amounted to a rate of approximately 0.67 degrees, while minimum temperatures decreased by a rate of 5.87 degrees over the previous period. Figure

(5a, b, c, and d) shows maps of the distribution of vegetation cover, precipitation, and maximum and minimum temperatures for Karbala Governorate.

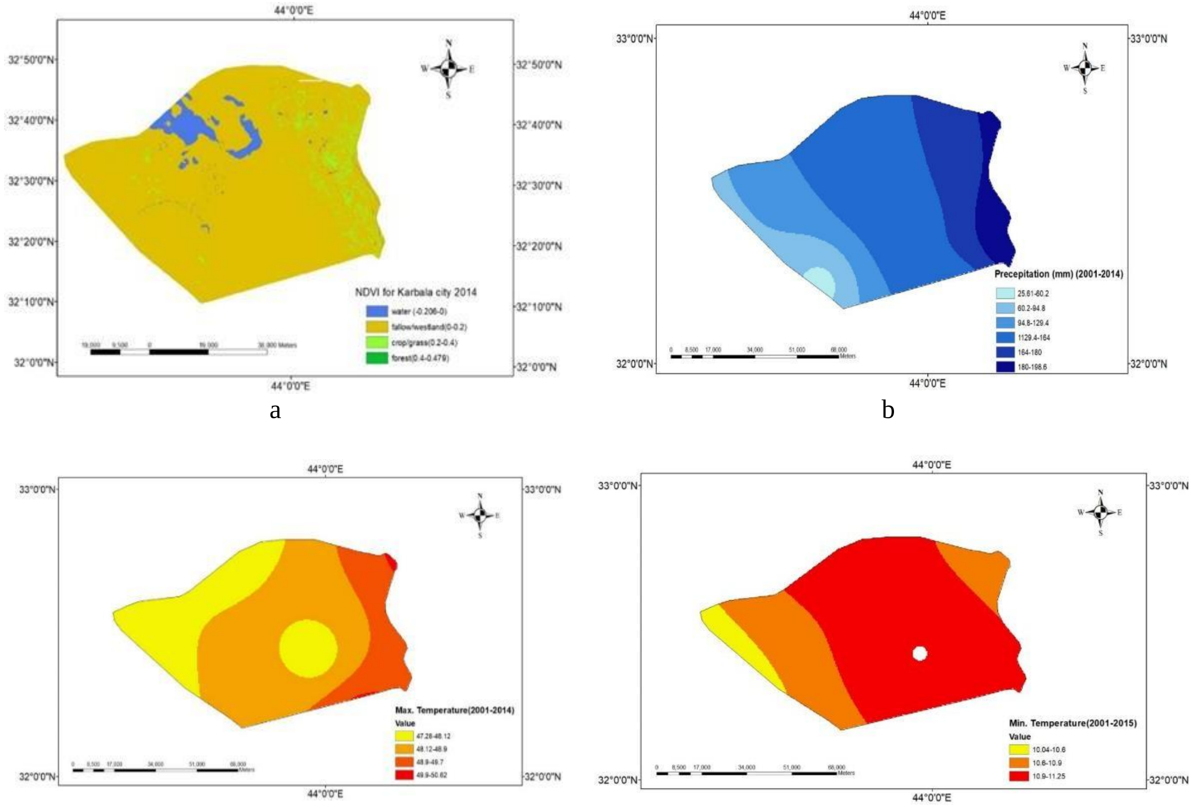

a b c d

Figure 5: (a, b, c, and d) the distribution of vegetation cover, precipitation, and maximum and minimum temperatures for Karbala Governorate.

4.1.3 For the Period (2015- January 2024):

For the period extending from 2015 to the end of January 2024, the results extracted by NDVI from the Land sat 8OLI satellite image showed the significant increase in vegetation cover, which increased at a significant rate of approximately 37,750 % over the previous period. The area, percentage, and other characteristics of vegetation cover during the period of 2015-February 2024 are displayed in table 4:

Table 4: Displayed the area, percentage of vegetation cover, and other characteristics during the (2015-February 2024)

Features	Area (km²)	% Percentage
Water	7.86879	4.775209
Wasteland / Fallow	130.17558	78.997605
Grass / Crop	16.7169	10.144722
Forest	10.02294	6.082464

This large increase in vegetation areas is due to several reasons, including the amounts of precipitation, which ranged at a rate between (87.87-136.5) mm for the period (2015-February 2024), meaning an increase of 274.4 % for the previous period The largest quantities were in the western part of the city. There are also projects to convert desert areas into green agricultural areas, which have been carried out since February 2020 by the Holy Abbasid Shrine, which consisted of planting wheat, and in November 2020, it began planting palm trees (https://al-wafifoundation.com/reading.php?id=320) there are seasonal plants such as crops (i.e, wheats, corns, etc.) and perennial plants such as palms. While during this period, the maximum and minimum temperatures increased at a rate of approximately 0.81 and 0.84 degrees Celsius, respectively. Figure (6 a, b, c, and d) shows maps of vegetation distribution, precipitation, and maximum and minimum temperatures, respectively.

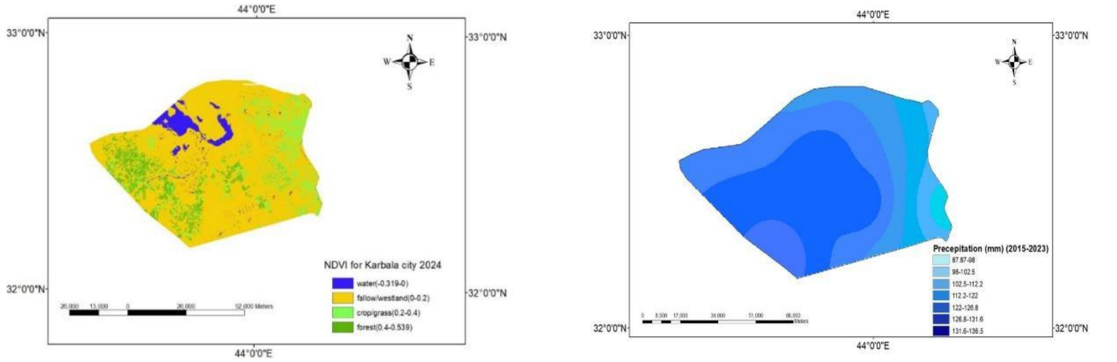

a b

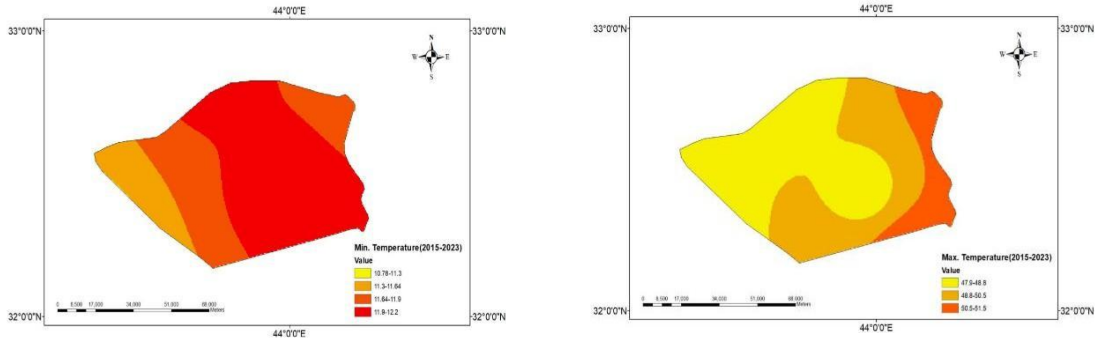

c d

Figure 6 (a, b, c, and d) shows maps of vegetation distribution, precipitation, and maximum and minimum temperatures, respectively

4.2 Effect of Climate Change on Vegetation Cover:

Using data from the HadGEM2-rcp26 climate model, the expected areas of vegetation cover were calculated based on the rates of increase or decrease in precipitation and compared with the increase or decrease in rainfall in the period from 2000-2024 and the areas of vegetation cover in this period through satellite images (7 ETM+ and 8 OLI). Two scenarios were studied, which include the first scenario is in the event that the Abbasid and Hussein shrines stop cultivating until the year 2024, while the second scenario includes if the shrines continue to cultivate for the coming years. Fig.7 shows precipitation data from the climate model HadGEM2-rcp26, as shown in the figure, it is shown that there is a decrease in precipitation amounts by 18-% for the period extending from (2024-2030), then this decrease increases for the period from (2031-2040) by 86% while precipitation amounts begin to increase by 104% for the periods from (2040-2050) and (2050-2060) and until the year 2070, the quantities decreased by 75-%, and increased 100% then the quantities decreased for the period extending to 2080 by -47%, while the maximum and minimum temperatures are close to the temperatures in the base period, as shown in the figure 8.

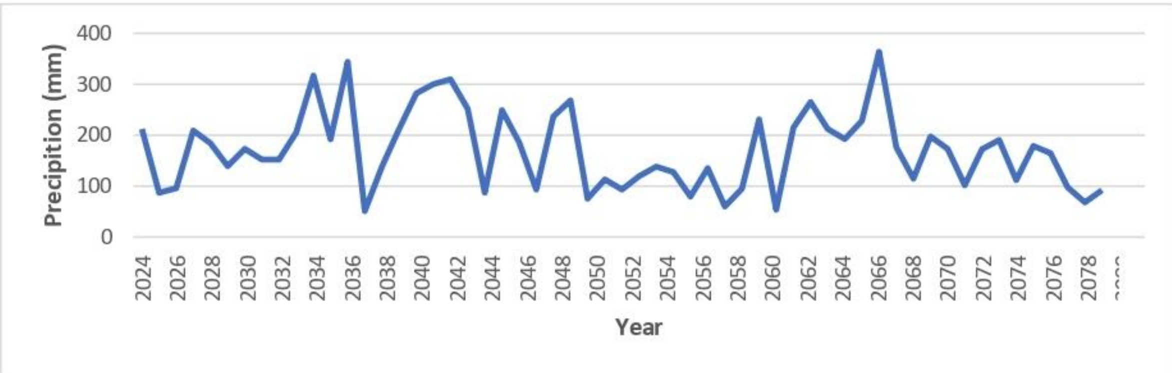

Figure 7: Precipitation under climate change for the period (20245-2080)

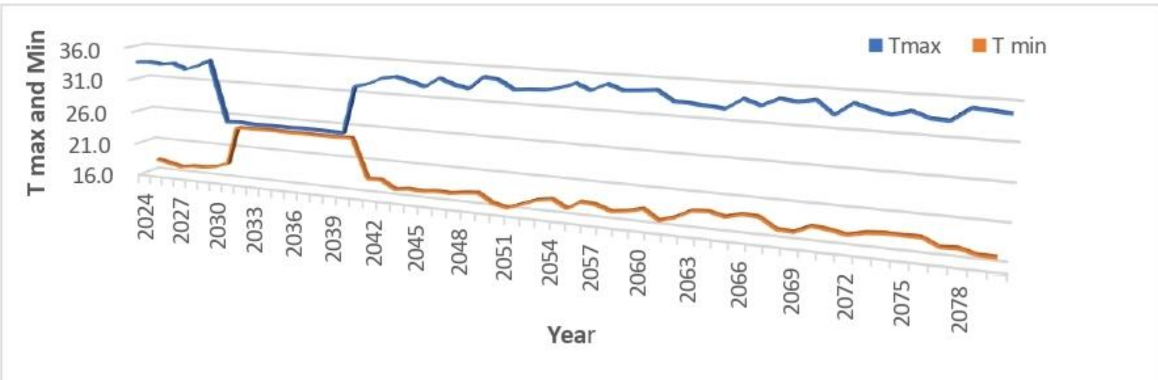

Figure 8: Annual average maximum and minimum temperature under climate change for the period (2024-2080)

4.2.1 Vegetation Cover Areas for Period (2024-2080):

The first scenario includes the event that the Abbasid and Hussein shrines stop cultivation to the extent currently present in the year 2024, and by studying the areas of vegetation cover in the base period with the precipitation rates in that period and comparing it with the quantities and rates of precipitation in the period from (2024-2050), it is expected that the vegetation cover will be by 2050 21.57 % as precipitation increases Projecting change in vegetation with change in climate, there is a decrease in percentage of vegetation in all period as shown in (Figure 9). Aggregated across the territory, the changes in vegetation simulated total from year 2024-2030 ,2031-2040, 2041-2050, 2051-2060, 2061-2070, and 2061-2070 are as follows: -7181450 %, -8083850 %, -6993450 %, -6391850 %, -4662250 %, and -4925450%. The largest decrease in vegetation occurs between years 2061-2070 and 2071-2080, but the smallest decrease occurs between 2031-2040.

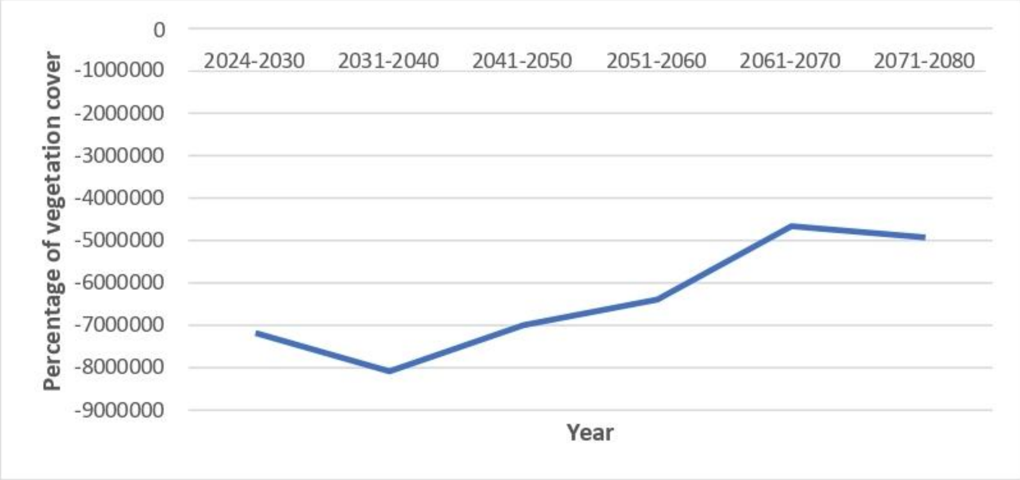

Figure 9: Vegetation forecasting under climate change for period (2024-2080)

5. Conclusions:

Vegetation cover is considered the basic base in the food pyramid for all living organisms. It is also considered one of the most important ecosystems because it contains all plant species, it reduces the effects of global warming by using solar energy to absorb carbon dioxide and provide the oxygen gas required for all species on Earth's surface to breathe. It also contributes to filtering and ridding the atmosphere of toxic gases and dust. Maintaining the appropriate temperature for life, and maintaining the cycles of mineral and organic elements in the soil and preventing the phenomena of erosion of soil.

The vegetation cover of the holy city of Karbala was calculated through NDVI for the years 2000, 2014, and 2024 in the month of February using Landsat satellite images (7 ETN+ and 8 OLI). The results indicated an increase in precipitation amounts by (153 %) during the period from year 2001 to year 2014, followed by an increase in vegetation cover areas by (245 %) then followed by an increase in precipitation amounts by (274.4 %) for the period from year 2015 to year 2024 with the projects of the Holy Abbasid Shrine to transform the Karbala desert into green spaces, which led to an increase in vegetation cover by (37,750 %).

For the future period, HadGEM2-rcp26 climate model was used, the amounts of precipitation for the period (2024-2050) decreased by 38%, while it increased by 372% for the period extending from (2050-2070), while for the period extending until the year 2080, the amounts of precipitation decreased by 47%.

The application of linear regression using Excel provided a straightforward method for predicting vegetation cover based on rainfall data. This approach not only facilitates understanding of the relationship between these variables but also supports future forecasting efforts.

References:

1. Prentice, I.C., Webb, R.S., Ter-Mikhaelian, M.T., Solomon, A.M., Smith, T.M., Pitovranov, S.E., et al. Developing a global vegetation dynamics model: results of an IIASA summer workshop. RR-89-7, International Institute for Applied System Analysis, Laxenburg, Austria; 1989.
2. Parry, M.L., Rosenzweig, C., Iglesias, A., Fischer, G., Livermore, M. The impacts of climate change on world agriculture: a synthesis. Nature 1988; 387-398.
3. Busby, J.R. Potential impacts of climate change on Australia's flora and fauna. Greenhouse 1988; 387-398.
4. Stepchenko, A., & Chizhov, J. NDVI short-term forecasting using recurrent neural networks. In: Environment. Technologies. Resources. Proceedings of the International Scientific and Practical Conference, Vol. 3, pp. 180-185; 2015.
5. Aman, A., Randriamanantena, H.P., Podaire, A., Frouin, R. Upscale integration of normalized difference vegetation index: The problem of spatial heterogeneity. IEEE Transactions on Geoscience and Remote Sensing 1992; 30(2): 326-338.
6. Hassan, W.H., Nile, B.K., Kadhim, Z.K., Mahdi, K., Riksen, M., Thiab, R.F. Trends, forecasting and adaptation strategies of climate change in the middle and west regions of Iraq. SN Applied Sciences 2023; 5(12): 312.
7. Mohammed, M.H., Zwain, H.M., Hassan, W.H. Modeling the impacts of climate change and flooding on sanitary sewage system using SWMM simulation: A case study. Results in Engineering 2021; 12: 100307.
8. Mohsen, K.A., Nile, B.K., Hassan, W.H. Experimental work on improving the efficiency of storm networks using a new galley design filter bucket. In: IOP Conference Series: Materials Science and Engineering, Vol. 671, No. 1, p. 012094; 2020.
9. Tucker, C.J., Miller, L.D., Pearson, R.L. Measurement of the combined effect of green biomass, chlorophyll, and leaf water on canopy spectro reflectance of the short grass prairie. Remote Sensing of Earth Resources; 1973.
10. Piao, S., Yin, G., Tan, J., Cheng, L., Huang, M., Li, Y., Wang, Y. Detection and attribution of vegetation greening trend in China over the last 30 years. Global Change Biology 2015; 21(4): 1601-1609.
11. Tang, Q., Vivoni, E.R., Muñoz-Arriola, F., Lettenmaier, D.P. Predictability of evapotranspiration patterns using remotely sensed vegetation dynamics during the North American monsoon. Journal of Hydrometeorology 2012; 13(1): 103-121.
12. Tsai, H.P., Yang, M.D. Relating vegetation dynamics to climate variables in Taiwan using 1982-2012 NDVI3g data. IEEE Journal of Selected Topics in Applied Earth Observations and Remote Sensing 2016; 9(4): 1624-1639.

13. Stocker, T.F., Qin, D., Plattner, G.K., Tignor, M., Allen, S.K., et al. The Physical Science Basis. Contribution of Working Group I to the Fifth Assessment Report of the Intergovernmental Panel on Climate Change. Cambridge University Press; 2013.
14. Birara, H., Pandey, R.P., Mishra, S.K. Projections of future rainfall and temperature using statistical downscaling techniques in Tana Basin, Ethiopia. Sustainable Water Resources Management 2020; 6(5): 77.
15. Rizvi, R.H., Yadav, R.S., Singh, R., Datt, K., Khan, I.A., Dhyani, S.K. Spectral analysis of remote sensing image for assessment of agro forestry areas in Yamunanagar district of Haryana. In: National Symposium on Advances in Geo-spatial Technologies with Special Emphasis on Sustainable Rainfed Agriculture, RRSSC, Nagpur; 2009.
16. Huete, A.R., Jackson, R.D., Post, D.F. Spectral response of a plant canopy with different soil backgrounds. Remote Sensing of Environment 1985; 17(1): 37-53.
17. Kshetri, T. NDVI, NDBI, and NDWI calculation using Landsat 7, 8. Geo World 2018; 2: 32-34.
18. Abdul-Razzak, M.I., Al-Neif, A.A.-A. The Quantitative and Qualitative Assessment of Groundwater in Karbala Governorate, Iraq. IOP Conference Series: Earth and Environmental Science 2022; 1080(1): 12013.
19. Al-Anbari, M.A., Ensaif, Y.R. Landfill Site Selection in Karbala Governorate, Iraq. Journal of Engineering and Sustainable Development 2018; 22(6): 30-42.
20. Al-Kaabi, M.A., Hmood, A.N. Study of the Radiological Doses in Karbala city. International Journal of Radiation Research 2019; 17(1): 171-176.
21. Khalaf, R.M., Hassan, W.H. Evaluation of irrigation water quality index IWQI for Al-Dammam confined aquifer in the west and southwest of Karbala city, Iraq. International Journal of Civil Engineering IJCE 2013; 23: 21-34.
22. Mohammed, E.A., Hani, Z.Y., Kadhim, G.Q. Assessing land cover/use changes in Karbala city (Iraq) using GIS techniques and remote sensing data. Journal of Physics: Conference Series 2018; 1032(1): 12047.
23. Kadhim, H., Mohammed, R. Analysis of NASA POWER Reanalysis Products to Predict Temperature and Precipitation in Euphrates River Basin. Journal of Hydrology 2023; 619: 129327.
24. Tayyeh, N., Mohammed, R. (2023). Title not provided in document.